Korean J. Chem. Eng., **29**(1), 111-119 (2012)
DOI: 10.1007/s11814-011-0129-y

Conductive chitosan/multi walled carbon nanotubes electrospun nanofiber feasibility

Zahra Moridi Mahdieh, Vahid Mottaghitalab, Negin Piri, and Akbar Khodaparast Haghi†

University of Guilan, P. O. Box 3756, Rasht 41635, Iran
(*Received 7 March 2011 • accepted 10 May 2011*)

Abstract−The current study focuses on the electrospinning of chitosan (CHT)/multi walled carbon nanotubes (MWNTs) composite nanofiber using a highly stable dispersion. The acetic acid (1-100%) and trifluoroacetic acid/dichloromethane (TFA/DCM 70 : 30) was tested as solvent, and the TFA/DCM (70 : 30) is most preferred for fiber formation process with acceptable electrospinnability. Moreover, a new protocol was used to establish proper technique for preparation of electrospinning solution. FT-IR spectroscopy utilized to infer the extent of interaction between CHT polymer chain and MWNT filaments. A quite simple technique was employed to show the stability of electrospinning solution before nanofiber formation process. Scanning electronic microscope (SEM) was employed to show the influence of spinning parameters on surface morphology of electrospun fiber. Under optimized condition, homogeneous and bead-free CHT/MWNTs nanofibers and known physical characteristics were prepared. The formation of conducting nanofibers based on CHT nanocomposites can be considered as a significant improvement in electrospinning of CHT/CNT dispersion. The direct outcome of the current study includes the homogeneous CHT/MWNTs nanofibers with an average diameter of 275 nm and a conductivity of 9×10^{-5} S/cm. These results are extremely important for further investigation regarding biomedical applications.

Key words: Biotechnology, MWNTs, Chitosan, Electrospinning, Biocomposite, Nanocomposite

INTRODUCTION

Over the recent decades, scientists have been interested in the creation of polymer nanofibers due to their potential in many engineering and medical applications [1]. According to various outstanding properties such as very small fiber diameters, large surface area per mass ratio, high porosity along with small pore sizes and flexibility, electrospun nanofiber mats have found numerous applications in diverse areas. For example, in the biomedical field nanofibers play a substantial role in tissue engineering [2], drug delivery [3], and wound dressing [4]. Electrospinning is a sophisticated and efficient method by which fibers are produced with diameters in nanometer scale entitled as nanofibers. In the electrospinning process, a strong electric field is applied on a droplet of polymer solution (or melt) held by its surface tension at the tip of a syringe needle (or a capillary tube). As a result, the pendent drop will become highly electrified and the induced charges distributes over its surface. Increasing the intensity of the electric field, the surface of the liquid drop will be distorted to a conical shape known as the Taylor cone [5]. Once the electric field strength exceeds a threshold value, the repulsive electric force dominates the surface tension of the liquid and a stable jet emerges from the cone tip. The charged jet then accelerates toward the target and rapidly thins and dries because of elongation and solvent evaporation. As the jet diameter decreases, the surface charge density increases and the resulting high repulsive forces split the jet to smaller jets. This phenomenon may take place several times leading to many small jets. Ultimately, solidification occurs and fibers deposit on the surface of the collector as a randomly oriented nonwoven mat [6,7]. Fig. 1 shows a schematic illustration of the electrospinning setup.

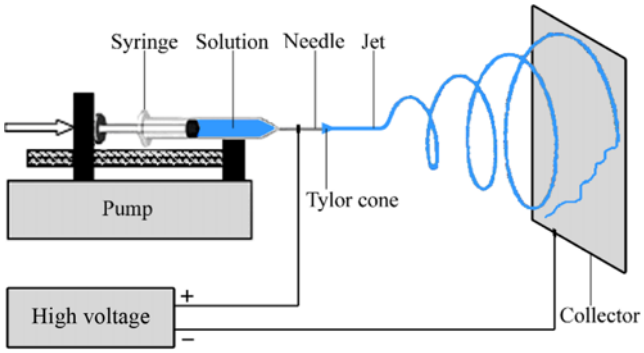

Fig. 1. A typical setup of the electrospinning process [8].

The physical characteristics of electrospun nanofibers such as fiber diameter depend on various parameters which are mainly divided into three categories: solution properties (solution viscosity, solution concentration, polymer molecular weight, and surface tension), processing conditions (applied voltage, volume flow rate, spinning distance, and needle diameter), and ambient conditions (temperature, humidity, and atmosphere pressure) [9]. Numerous applications require nanofibers with desired properties, suggesting the importance of process control. It does not come true unless having a comprehensive outlook of the process and quantitative study of the effects of governing parameters. In this context, Sukigara et al. [10] assessed the effect of concentration on diameter of electrospun nanofibers.

Beside physical characteristics, medical scientists have shown a remarkable attention to biocompatibility and biodegradability of nano-

†To whom correspondence should be addressed.
E-mail: Haghi@Guilan.ac.ir, AKHaghi@yahoo.com

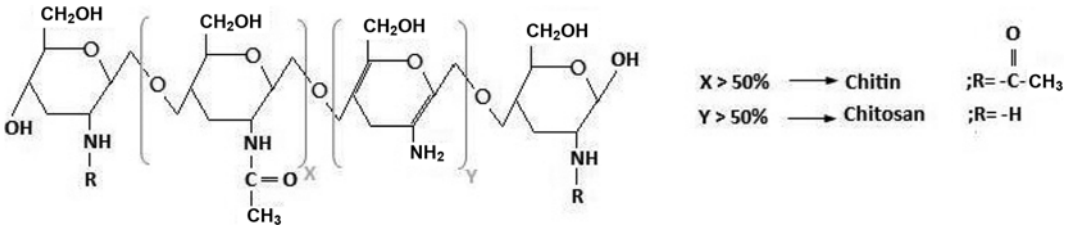

Scheme 1. Chemical structures of chitin and chitosan biopolymers.

fibers made of biopolymers such as collagen [11], fibrogen [12], gelatin [13], silk [14], chitin [15] and chitosan [16]. Chitin is the second-most abundant natural polymer in the world and Chitosan (poly-(1-4)-2-amino-2-deoxy-β-D-glucose) is the deacetylated product of chitin [17]. CHT is well known for its biocompatible and biodegradable properties [18].

Chitosan (CHT) is insoluble in water, alkali, and most mineral acidic systems. However, though its solubility in inorganic acids is quite limited, CHT is in fact soluble in organic acids, such as dilute aqueous acetic, formic, and lactic acids. CHT also has free amino groups, which makes it a positively charged polyelectrolyte. This property makes CHT solutions highly viscous and complicates its electrospinning [19]. Furthermore, the formation of strong hydrogen bonds in a 3-D network prevents the movement of polymeric chains exposed to the electrical field [20].

Different strategies were used for bringing chitosan in nanofiber form. The three top most abundant techniques include blending of favorite polymers for electrospinning process with CHT matrix [21, 22], alkali treatment of CHT backbone to improve electro spinnability through reducing viscosity [23] and employment of concentrated organic acid solution to produce nanofibers by decreasing of surface tension [24]. Electrospinning of polyethylene oxide (PEO)/CHT [21] and polyvinyl alcohol (PVA)/CHT [22] blended nanofiber are two recent studies based on first strategy. In the second protocol, the molecular weight of chitosan decreases through alkali treatment. Solutions of the treated chitosan in aqueous 70-90% acetic acid produce nanofibers with appropriate quality and processing stability [23].

Using concentrated organic acids such as acetic acid [24] and triflouroacetic acid (TFA) with and without dichloromethane (DCM) [25,26] has been reported exclusively for producing neat CHT nanofibers. They similarly reported the decreasing of surface tension and at the same time enhancement of charge density of CHT solution without significant effect on viscosity. This new method suggests significant influence of the concentrated acid solution on the reducing of the applied field required for electrospinning.

The mechanical and electrical properties of neat CHT electrospun natural nanofiber mat can be improved by addition of the synthetic materials including carbon nanotubes (CNTs) [27]. CNTs are one of the important synthetic polymers that were discovered by Iijima in 1991 [28]. CNTs, either single-walled nanotubes (SWNTs) or multiwalled nanotubes (MWNTs), combine the physical properties of diamond and graphite. They are extremely thermally conductive like diamond and appreciably electrically conductive like graphite. Moreover, the flexibility and exceptional specific surface area to mass ratio can be considered as significant properties of CNTs [29]. Scientists are becoming more interested in CNTs for existence of exclusive properties such as superb conductivity [30] and mechanical strength for various applications. To the best of our knowledge, there has been no report on electrospinning of CHT/MWNTs blend, except those [30,31] that use PVA to improve spinnability. Results showed uniform and porous morphology of the electrospun nanofibers. Despite adequate spinnability, total removing of PVA from nanofiber structure to form conductive substrate is not feasible. Moreover, thermal or alkali solution treatment of CHT/PVA/MWNTs nanofibers extremely influence on the structural morphology and mechanical stiffness. The CHT/CNT composite can be produced by the hydrogen bonds due to hydrophilic positively charged polycation of CHT due to amino groups and hydrophobic negatively charged of CNT due to carboxyl and hydroxyl groups [32-34].

In the current study, we have attempted to produce a CHT/MWNTs nanofiber without association of processing agent to facile electrospinng process. In addition, a new approach was explored to provide highly stable and homogeneous composite spinning solution of CHT/MWNTs in concentrated organic acids. This in turn presents a homogenous conductive CHT scaffolds which is extremely important for biomedical implants.

EXPERIMENTAL

1. Materials

CHT with degree of deacetylation of 85% and molecular weight of 5×10^5 was supplied by Sigma-Aldrich. The MWNTs, supplied by Nutrino, have an average diameter of four nm and purity of about 98%. All of the other solvents and chemicals were commercially available and used as received without further purification.

2. Preparation of CHT-MWNTs Dispersions

A Branson Sonifier 250 operated at 30 W used to prepare the MWNT dispersions in CHT/organic acid (90%wt acetic acid, 70/30 TFA/DCM) solution based on different protocols. In the first approach, 3 mg of as received MWNTs was dispersed into deionized water or DCM using solution sonicating for 10 min (current work, sample 1). Different amount of CHT was then added to MWNTs dispersion for preparation of a 8-12 wt% solution and then sonicated for another 5 min. Fig. 2 shows two different protocols used in this study.

In the next step, organic acid solution was added to obtain a CHT/MWNT solution with total volume of 5 mL and finally the dispersion was stirred for another 10 hours. Sample 2 was prepared using the second technique. Same amount of MWNTs was dispersed in CHT solution, and the blend with total volume of 5 mL was sonicated for 10 min and dispersion was stirred for 10 hr [35].

3. Electrospinning of CHT/MWNT Dispersion

After the preparation of spinning solution, it was transferred to a

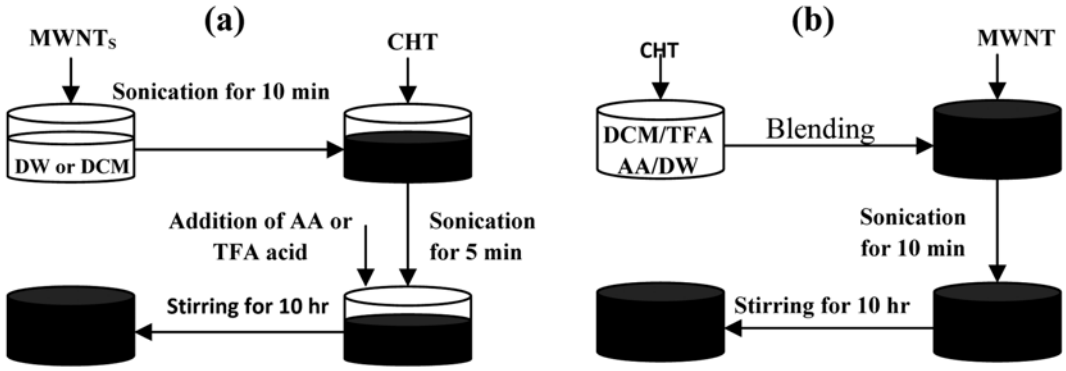

Fig. 2. Two protocols used in this study for preparation of MWNTs/CHT dispersion (a) current study (b) ref. [35].

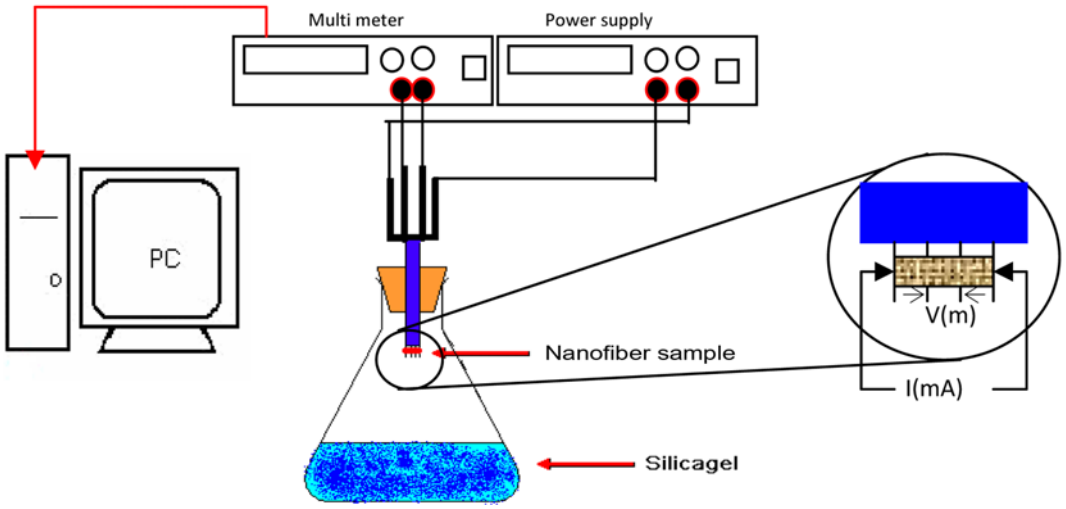

Fig. 3. The experimental setup for four-probe electrical conductivity measurement of nanofiber thin film.

5 mL syringe and became ready for spinning of nanofibers. The experiments carried out on a horizontal electrospinning setup are shown schematically in Fig. 1. The syringe containing CHT/MWNTS solution was placed on a syringe pump (New Era NE-100) used to dispense the solution at a controlled rate. A high voltage DC power supply (Gamma High Voltage ES-30) was employed to generate the required electric field for electrospinning. The positive electrode and the grounding electrode of the high voltage supplier attached, respectively, to the syringe needle and flat collector wrapped with aluminum foil where electrospun nanofibers accumulates via an alligator clip to form a nonwoven mat. The voltage and the tip-to-collector distance fixed, respectively, on 18-24 kV and 4-10 cm. In addition, the electrospinning was carried out at room temperature and the aluminum foil was removed from the collector.

4. Measurements and Characterizations Method

A small piece of mat was placed on the sample holder and gold sputter-coated (Bal-Tec). Thereafter, the micrograph of electrospun CHT/MWNT fibers was obtained using scanning electron microscope (SEM, Phillips XL-30). Fourier transform infrared spectra (FTIR) were recorded using a Nicolet 560 spectrometer to investigate the interaction between CHT and MWNT in the range of 800-4,000 cm^{-1} under a transmission mode. The size distribution of the dispersed solution was evaluated with a Zetasizer (Malvern Instruments). The conductivity of nanofiber samples was measured with a homemade four-probe electrical conductivity cell operating at constant humidity. The electrodes were circular pins with separation distance of 0.33 cm and fibers connected to pins by silver paint (SPI). Between the two outer electrodes, a constant DC current was applied by Potentiostat/Galvanostat model 363 (Princeton Applied Research). The generated potential difference between the inner electrodes and the current flow was recorded by digital multimeter 34401A (Agilent). Fig. 3 illustrates the experimental setup for conductivity measurement. The conductivity (δ: S/cm) of the nanofiber thin film with rectangular surface can then be calculated according to Eq. (1), which parameters call for length (L: cm), width (W: cm), thickness (t: cm), DC current applied (mA) and the potential drop across the two inner electrodes (mV). All measuring was repeated at least five times for each set of samples.

$$\delta = \frac{I \times L}{V \times W \times t} \quad (1)$$

RESULTS AND DISCUSSION

1. The Characteristics of MWNT/CHT Dispersion

Utilization of MWNTs in biopolymer matrix initially requires

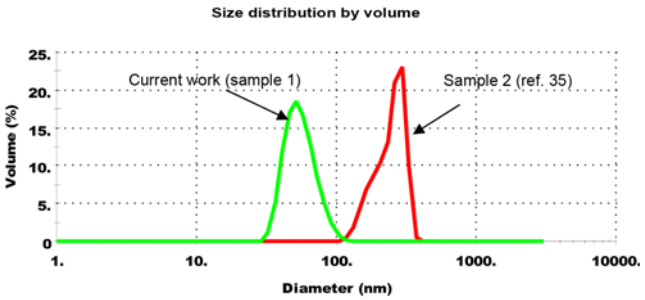

Fig. 4. Hydrodynamic diameter distribution of MWNT bundles in CHT/acetic acid (1%) solution for different preparation technique.

their homogeneous dispersion in a solvent or polymer matrix. Dynamic light scattering (DLS) is a sophisticated technique used for evaluation of particle size distribution. DLS provides many advantages for particle size analysis to measure a large population of particles in a very short time period, with no manipulation of the surrounding medium. Dynamic light scattering of MWNTs dispersions indicates that the hydrodynamic diameter of the nanotube bundles is between 150 and 400 nm after 10 min of sonication for sample 2 (Fig. 4).

MWNTs bundle in sample 1 (different approach but same sonication time compared to sample 2) shows a range of hydrodynamic diameter between 20-100 nm (Fig. 4). The lower range of hydrodynamic diameter for sample 1 correlates to more exfoliated and highly stable nanotubes strands in CHT solution. The higher stability of sample 1 compared to sample 2 over a long period of time is confirmed by solution stability test. The results presented in Fig. 5 indicate that procedure employed for preparation of sample 1 (current work) was an effective method for dispersing MWNTs in CHT/acetic acid solution. However, MWNTs bundles in sample 2 were found to re-agglomerate upon standing after sonication, as shown in Fig. 5 which indicates the sedimentation of large agglomerated particles.

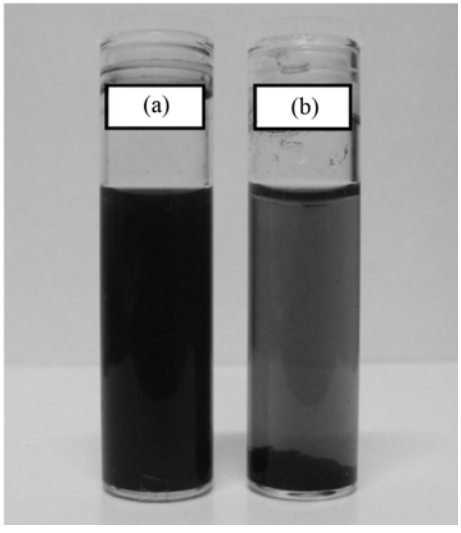

Fig. 5. Stability of CHT-MWNT dispersions (a) current work (sample 1) (b) ref. [35] (sample 2).

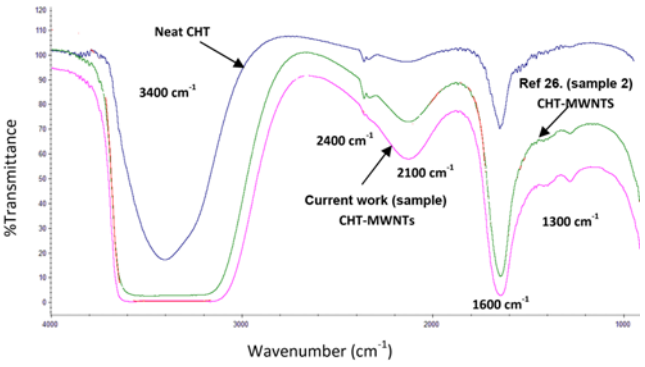

Fig. 6. FTIR spectra of CHT-MWCNT in 1% acetic acid with different techniques of dispersion.

Despite the method reported in ref 35, neither sedimentation nor aggregation of the MWNTs bundles was observed in the first sample. Presumably, this behavior in sample 1 can be attributed to contribution of CHT biopolymer to forming an effective barrier against re-agglomeration of MWNTs nanoparticles. In fact, using sonication energy, in the first step without presence of solvent, makes very tiny exfoliated but unstable particle in water as dispersant. Instantaneous addition of acetic acid as solvent and long mixing most likely helps the wrapping of MWNTs strands with CHT polymer chain.

Fig. 6 shows the FTIR spectra of neat CHT solution and CHT/MWNTs dispersions prepared using strategies explained in the experimental part. The interaction between the functional group associated with MWNTs and CHT in dispersed form have been understood through recognition of functional groups. The enhanced peaks at ~1,600 cm^{-1} can be attributed to (N-H) band and (C=O) band of amid functional group. However, the intensity of amid group for CHT/MWNTs dispersion increases presumably due to contribution of G band in MWNTs. More interestingly, in this region, the FTIR spectra of MWNTs-CHT dispersion (sample 1) have been highly intensified compared to sample 2 [35]. It correlates to higher chemical interaction between acid functionalized C-C group of MWNTs and amid functional group in CHT.

This probably is the main reason of the higher stability and lower MWNTs dimension demonstrated in Fig. 4 and Fig. 5. Moreover, the intensity of protonated secondary amine absorbance at 2,400 cm^{-1} for sample 1 prepared by new technique is negligible compared to sample 2 and neat CHT. Furthermore, the peak at 2,123 cm^{-1} is a characteristic band of the primary amine salt, which is associated with the interaction between positively charged hydrogen of acetic acid and amino residues of CHT. In addition, the broad peaks at ~3,410 cm^{-1} are due to the stretching vibration of OH group superimposed on NH stretching bond and broadened due to hydrogen bonds of polysaccharides. The broadest peak of hydrogen bonds was observed at 3,137-3,588 cm^{-1} for MWNTs/CHT dispersion prepared by new technique (sample 1).

2. The Physical and Morphological Characteristics of MWNTs/CHT Nanofiber

Different solvents including acetic acid 1-90%, pure formic acid, and TFA/DCM were tested for preparation of spinning solution using the protocol explained for sample 1. Upon applying of the high voltage even above 25 kV no polymer jet formed using acetic acid 1-30% and formic acid as the solvent for chitosan/carbon nanotube.

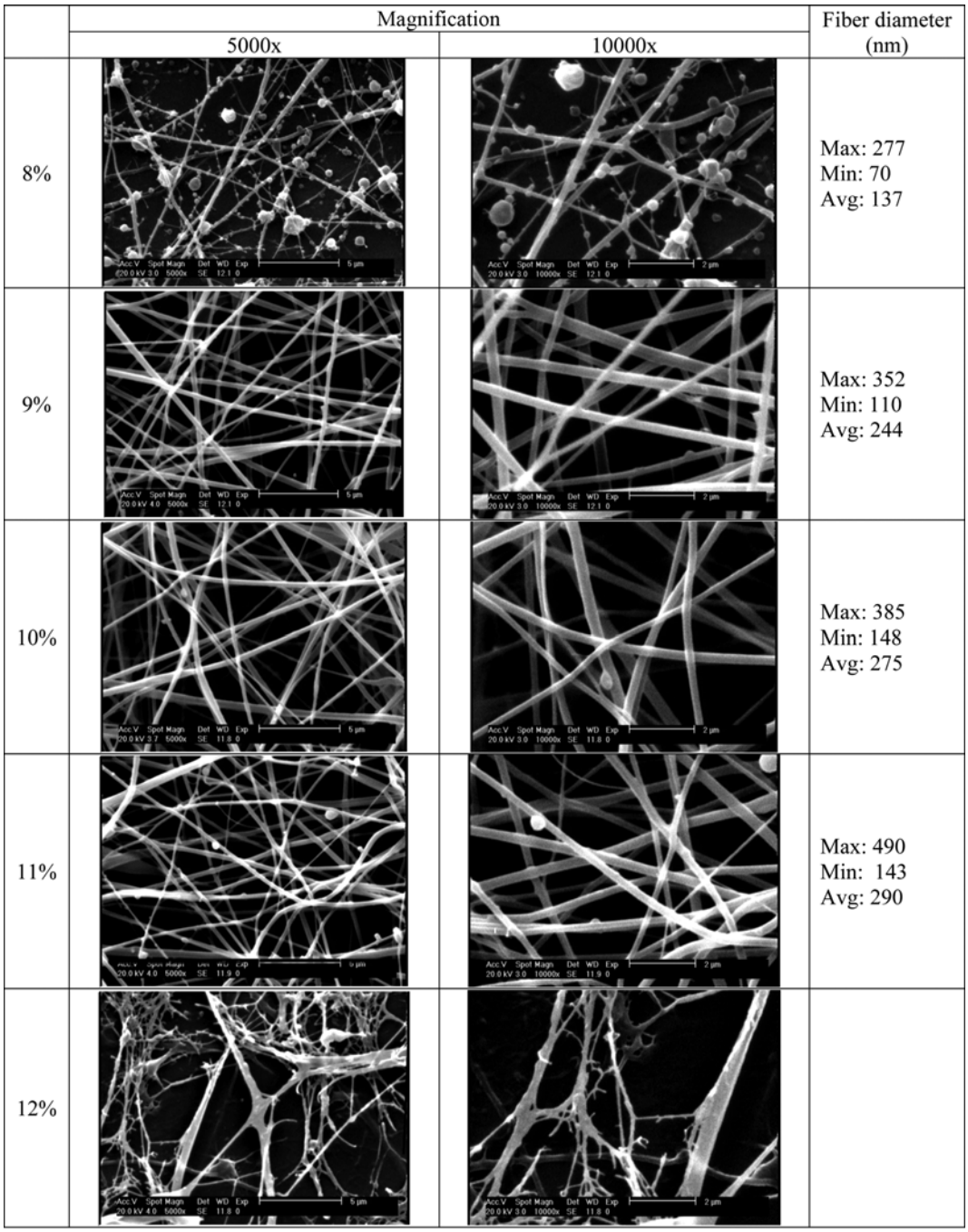

Fig. 7. Scanning electron micrographs of electrospun nanofibers at different CHT concentration (wt%): (a) 8, (b) 9, (c) 10, (d) 11, (e) 12, 24 kV, 5 cm, TFA/DCM: 70/30, (0.06%wt MWNTs).

However, experimental observation shows bead formation when acetic acid (30-90%) was used as the solvent. Therefore, one does not expect the formation of electrospun fiber of MWNT/CHT using prescribed solvents (data not shown).

Fig. 7 shows scanning electronic micrographs of the MWNTs/CHT electrospun nanofibers in different concentration of CHT in TFA/DCM (70 : 30) solvent. As presented in Fig. 7(a), at low concentrations of CHT the beads deposited on the collector and thin fibers co-existed among the beads. When the concentration of CHT increases as shown in Fig. 7(a)-(c) the bead density decreases. Fig. 7(c) shows homogeneous electrospun nanofibers with minimum beads, thin and interconnected fibers. More increasing of concentration of CHT led to increasing of interconnected fibers at Fig. 7(d)-(e). Fig. 8 shows the effect of concentration on average diameter of MWNTs/CHT electrospun nanofibers. Our assessments indicate that the fiber diameter of MWNTs/CHT increases with the increasing of the CHT concentration. In this context, similar results were reported in previously published work [36-37]. Hence, MWNTs/CHT (10%wt) solution in TFA/DCM (70 : 30) considered as resulting as optimized concentration. An average diameter of 275 nm (Fig. 7(c): diameter distribution, 148-385) was investigated for these conditions. Table 1 lists the variation of nanofiber diameter and four

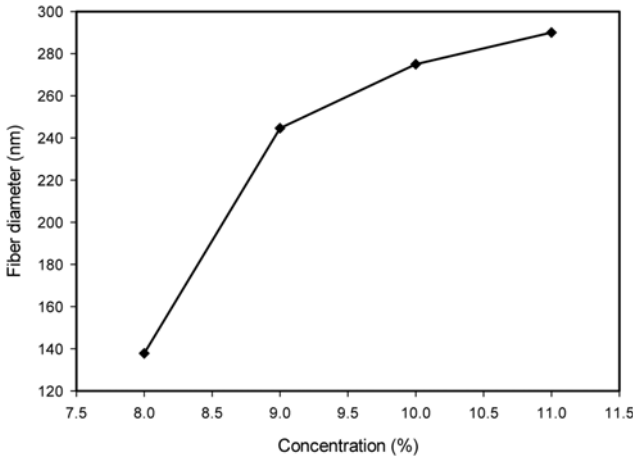

Fig. 8. The effect of the CHT concentration in CHT/MWNT dispersion on nanofiber diameter.

probe electrical conductivity based on the different loading of CHT. One can expect lower conductivity once the CHT content increases. However, the higher the CHT concentration, the thinner fiber forms. Therefore, the decreasing of conductivity at higher CHT concentration damps by decreasing of nanofiber diameter. This led to a nearly constant conductivity over entire measurements.

Fig. 9 shows the influence of voltage on morphology of CHT/MWNT electrospun nanofibers acquired SEM images. In our experiments, 18 kV attains as threshold voltage, where fiber formation occurs.

For lower voltage, the beads and some little fiber are deposited on the collector (Fig. 9(a)). As shown in Fig. 9(a)-(d), the beads decrease while voltage is increasing from 18 kV to 24 kV. The collected nanofibers by applying 18 kV (9a) and 20 kV (9b) were not quite clear and uniform. The higher the applied voltage, uniform nanofibers with narrow distribution start to form. The average diameter of fibers, 22 kV (9c), and 24 kV (9d), respectively, was 204 (79-391), and 275 (148-385). The conductivity measurement given in Table 2 confirms our observation in the first set of conductivity data. As can be seen from the last row, the amount of electrical conductivity reaches a maximum level of 9×10^{-5} at prescribed setup.

The distance between tips to collector is another parameter that

Table 1. The variation of conductivity and mean nanofiber diameter versus chitosan loading

% CHT (%w/v)	% MWNT (%w/v)	Voltage (KV)	Tip to collector (cm)	Diameter (nm)	Conductivity (S/cm)
8	0.06	24	5	137±58	NA
9	0.06	24	5	244±61	9×10^{-5}
10	0.06	24	5	275±70	9×10^{-5}
11	0.06	24	5	290±87	8×10^{-5}
12	0.06	24	5	Non uniform	NA

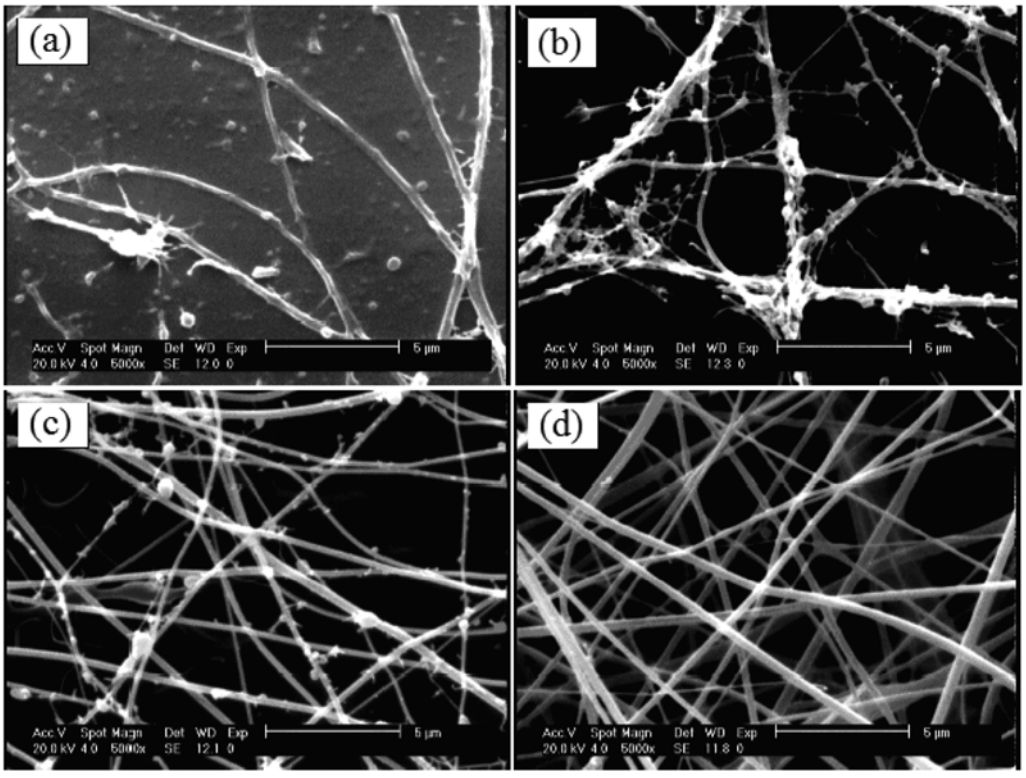

Fig. 9. Scanning electronic micrographs of electrospun fibers at different voltage (kV): (a) 18, (b) 20, (c) 22, (d) 24, 5 cm, 10 wt%, TFA/DCM: 70/30. (0.06%wt MWNTs).

Table 2. The variation of conductivity and mean nanofiber diameter versus applied voltage

% CHT (%w/v)	% MWNT (%w/v)	Voltage (KV)	Tip to collector (cm)	Diameter (nm)	Conductivity (S/cm)
10	0.06	18	5	Non uniform	NA
10	0.06	20	5	Non uniform	NA
10	0.06	22	5	201±66	6×10^{-5}
10	0.06	24	5	275±70	9×10^{-5}

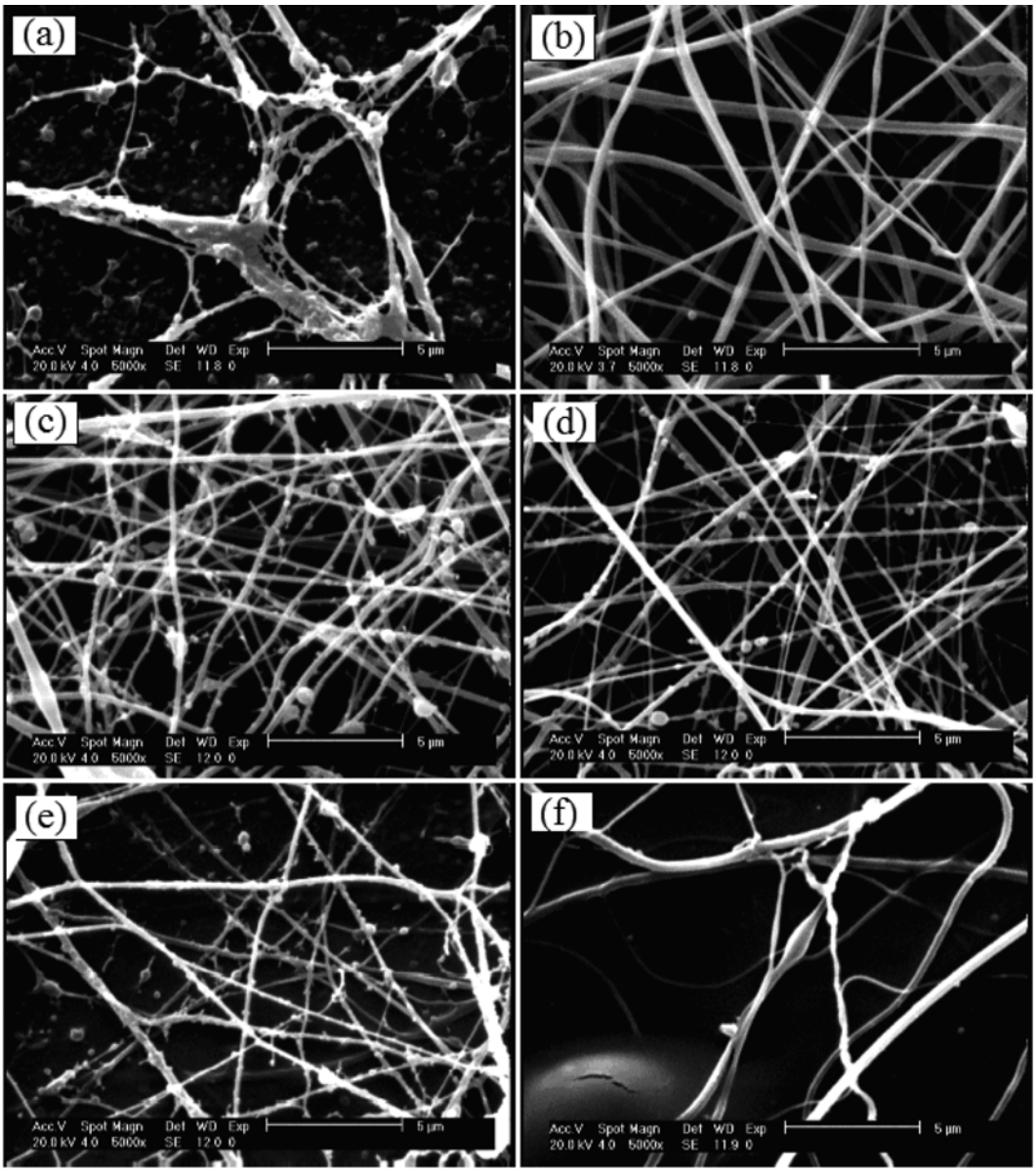

Fig. 10. Scanning electronic micrographs of electrospun fibers of Chitosan/Carbon nanotubes at different tip-to-collector distances (cm): (a) 4, (b) 5, (c) 6, (d) 7, (e) 8, (f) 10, 24 kV, 10 wt%, TFA/DCM: 70/30.

controls the fiber diameter and morphology. Fig. 10 shows the change in morphologies of CHT/MWNTs electrospun nanofibers at different distance. When the distance is not long enough, the solvent could not find opportunity to be separated, hence, the interconnected thick nanofiber deposits on the collector (Fig. 10(a)). However, the adjusting of the distance on 5 cm (Fig. 10(b)) leads to homogeneous nanofibers with negligible beads and interconnected areas. However, the beads increase by increasing of distance of the tip-to-collector as represented from Fig. 10(b) to 10(f). Similar results were observed for CHT nanofibers reported by Geng et al. [24]. Also, the results show that the diameter of electrospun fibers decreases by increasing of distance tip to the collector in Fig. 10(b), 10(c), 10(d), respectively, 275 (148-385), 170 (98-283), 132 (71-224). Similarly, the previous works report a decreasing trend in nanofiber diam-

Table 3. The variation of conductivity and mean nanofiber diameter versus applied voltage

% CHT (%w/v)	% MWNT (%w/v)	Voltage (KV)	Tip to collector (cm)	Diameter (nm)	Conductivity (S/cm)
10	0.06	24	4	Non uniform	NA
10	0.06	24	5	275±70	9×10^{-5}
10	0.06	24	6	170±58	6×10^{-5}
10	0.06	24	7	132±53	7×10^{-5}
10	0.06	24	8	Non uniform	NA
10	0.06	24	10	Non uniform	NA

eter once distance increases [38,39]. A remarkable defect and non-homogeneity appears for those fibers prepared at a distance of 8 cm (Fig. 10(e)) and 10 cm (Fig. 10(f)). However, a 5 cm distance was selected as the proper amount for CHT/MWNT electrospinning process. Conductivity results also are in agreement with those data obtained in previous parts (Table 3).

The non-homogeneity and huge bead densities act as a barrier against electrical current and still a bead-free and thin nanofiber mat shows higher conductivity compared to other samples. Experimental framework in this study was based on parameter adjusting for electrospinning of conductive CHT/MWNTs nanofiber. It can be expected that the addition of nanotubes can boost conductivity and change morphological aspects, which is extremely important for biomedical applications.

CONCLUSIONS

Conductive composite nanofiber of CHT/MWNTs was produced using conventional electrospinning technique. A new protocol is suggested for preparation of electrospinning solution, which shows much better stability and homogeneity compared to previous techniques. Several solvent including acetic acid 1-90%, formic acid, and TFA/DCM (70 : 30) were investigated in the electrospinning of CHT/MWNTs dispersion. Using DLS and dispersion stability tests showed that the TFA/DCM (70 : 30) solvent is most preferred for nanofiber formation process with acceptable electrospinnability. The formation of nanofibers with conductive pathways regarding to exfoliated and interconntected nanotube strands is a breakthrough in chitosan nanocomposite area. This is a significant improvement in electrospinning of chitosan/carbon nanotube dispersion. It has been also observed that the homogeneous nanofibers with an average diameter of 275 nm could be prepared with a conductivity of 9×10^{-5}.

ACKNOWLEDGEMENT

Authors would like to acknowledge Guilan Science and Technology Park (GSTP) for their technical and financial supports.

REFERENCES

1. S. Agarwal, J. H. Wendorff and A. Greiner, *Polymer*, **49**, 5603 (2008).
2. M. Li, M. J. Mondrinos, M. R. Gandhi, F. K. Ko, A. S. Weiss and P. I. Lelkes, *Biomaterials*, **26**, 5999 (2005).
3. J. Zeng, L. Yang, Q. Liang, X. Zhang, H. Guan, X. Xu, X. Chen and X. Jing, *J. Control. Release*, **105**, 43 (2005).
4. M.-S. Khil, D.-I. Cha, H.-Y. Kim, I.-S. Kim and N. Bhattarai, *J. Biomed. Mat. Res. B.*, **67B**, 675 (2003).
5. G. I. Taylor, *Proc. Roy. Soc. London*, **313**, 453 (1969).
6. J. Doshi and D. H. Reneker, *J. Electrostat.*, **35**, 151 (1995).
7. D. Li and Y. Xia, *Adv. Mater.*, **16**, 1151 (2004).
8. M. Ziabari, V. Mottaghitalab and A. K. Haghi, *Korean J. Chem. Eng.*, **25**, 923 (2008).
9. S. H. Tan, R. Inai, M. Kotaki and S. Ramakrishna, *Polymer*, **46**, 6128 (2005).
10. S. Sukigara, M. Gandhi, J. Ayutsede, M. Micklus and F. Ko, *Polymer*, **44**, 5721 (2003).
11. J. A. Matthews, G. E. Wnek, D. G. Simpson and G. L. Bowlin, *Biomacromolecules*, **3**, 232 (2002).
12. M. C. McManus, E. D. Boland, D. G. Simpson, C. P. Barnes and G. L. Bowlin, *J. Biomed. Mater. Res. A.*, **81A**, 299 (2007).
13. Z.-M. Huang, Y. Z. Zhang, S. Ramakrishna and C. T. Lim, *Polymer*, **45**, 5361 (2004).
14. X. Zhang, M. R. Reagan and D. L. Kaplan, *Adv. Drug. Del. Rev.*, **61**, 988 (2009).
15. H. K. Noh, S. W. Lee, J.-M. Kim, J.-E. Oh, K.-H. Kim, C.-P. Chung, S.-C. Choi, W. H. Park and B.-M. Min, *Biomaterials*, **27**, 3934 (2006).
16. K. Ohkawa, K.-I. Minato, G. Kumagai, S. Hayashi and H. Yamamoto, *Biomacromolecules*, **7**, 3291 (2006).
17. O. C. Agboh and Y. Qin, *Polym. Adv. Technol.*, **8**, 355 (1997).
18. M. Rinaudo, *Prog. Polym. Sci.*, **31**, 603 (2006).
19. I. Aranaz, M. Mengíbar, R. Harris, I. Paños, B. Miralles, N. Acosta, G. Galed and Á. Heras, *Curr. Chem. Biol.*, **3**, 203 (2009).
20. A. Neamnark, R. Rujiravanit and P. Supaphol, *Carbohydr. Polym.*, **66**, 298 (2006).
21. B. Duan, C. Dong, X. Yuan and K. Yao, *J. Biomater. Sci. Polym. Ed.*, **15**, 797 (2004).
22. Y.-T. Jia, J. Gong, X.-H. Gu, H.-Y. Kim, J. Dong and X.-Y. Shen, *Carbohydr. Polym.*, **67**, 403 (2007).
23. H. Homayoni, S. A. H. Ravandi and M. Valizadeh, *Carbohydr. Polym.*, **77**, 656 (2009).
24. X. Geng, O.-H. Kwon and J. Jang, *Biomaterials*, **26**, 5427 (2005).
25. S. Torres-Giner, M. J. Ocio and J. M. Lagaron, *Anglais*, **8**, 303 (2008).
26. S. D. Vrieze, P. Westbroek, T. V. Camp and L. V. Langenhove, *J. Mater. Sci.*, **42**, 8029 (2007).
27. K. Ohkawa, D. Cha, H. Kim, A. Nishida and H. Yamamoto, *Macromol. Rapid Commun.* , **25**, 1600 (2004).
28. S. Iijima, *Nature*, **354**, 56 (1991).
29. A. M. K. Esawi and M. M. Farag, *Mater. Design*, **28**, 2394 (2007).

30. W. Feng, Z. Wu, Y. Li, Y. Feng and X. Yuan, *Nanotechnology*, **19**, 105707 (2008).
31. H. Liao, R. Qi, M. Shen, X. Cao, R. Guo, Y. Zhang and X. Shi, *Colloid. Surface. B.*, doi:10.1016/j.colsurfb.2011.02.010 (2011).
32. S.-H. Baek, B. Kim and K.-D. Suh, *Colloid. Surface. A.*, **316**, 292 (2008).
33. Y.-L. Liu, W.-H. Chen and Y.-H. Chang, *Carbohydr. Polym.*, **76**, 232 (2009).
34. J. Tkac, J. W. Whittaker and T. Ruzgas, *Biosens. Bioelectron.*, **22**, 1820 (2007).
35. G. M. Spinks, M. Geoffrey, S. R. Shin, G. G. Wallace, P. G. Whitten, S. I. Kim and S. J. Kim, *Sensor. Actuat. B-Chem.*, **115**, 678 (2006).
36. H. Zhang, Z. Wang, Z. Zhang, J. Wu, J. Zhang and J. He, *Adv. Mater.*, **19**, 698 (2007).
37. J. M. Deitzel, J. Kleinmeyer, D. Harris and N. C. Beck Tan, *Polymer*, **42**, 261 (2001).
38. S. Zhang, W. S. Shim and J. Kim, *Mater. Design*, **30**, 3659 (2009).
39. Y. Li, Z. Huang and Y. Lu, *Eur. Polym. J.*, **42**, 1696 (2006).